

# Activation energy spectra and relaxation in amorphous materials

M. R. J. GIBBS, J. E. EVETTS, J. A. LEAKE

*Department of Metallurgy and Materials Science, University of Cambridge, Pembroke Street, Cambridge, UK*

A theoretical model for relaxation in glassy materials, in particular metallic glasses, based on a spectrum of available processes distributed in activation energy is presented. The model is used to discuss “ln  $t$ ” kinetics, “reversibility” and “crossover” effects which have been observed experimentally. Where direct comparison is possible between the theory and experiment the agreement is good over all these various observed phenomena.

## 1. Introduction

It is now well established that glasses are metastable with respect to crystallization, and also to structural relaxation within an amorphous phase. This second form of metastability, the subject of this paper, is a direct consequence of the rapid solidification process used to produce the glass, and has been found to have considerable influence on the measured value of many physical properties. Although this work has arisen from a study of metallic glasses, and much of the data discussed is on such systems, the approach to relaxation given below is applicable to any amorphous material.

The measured physical property/time/temperature behaviour of glasses is a complex function of thermo-mechanical history from the moment of solidification until the time of measurement of the physical property. Three main phenomena have been commonly described in previous studies of relaxation in metallic glasses. When the change in the measured property varies linearly with the logarithm of the isothermal annealing time “ln  $t$ ” kinetics are said to be obeyed. “Reversibility” has been seen when the value of a measured physical property is first of all made to vary little with time by annealing at one temperature, and then the annealing temperature is changed. The measured property now tends to a different value (again approximately constant with respect to time) characteristic of the new annealing temperature; the temperature can often be cycled several times, with corresponding changes in the

measured property, before crystallization occurs. The “crossover” effect is illustrated in Fig. 1. Annealing at temperature  $T_{a_1}$  causes the property  $P$  to change as shown. If the experiment is stopped after time  $t_1$  and the temperature stepped to  $T_{a_2}$  ( $T_{a_2} > T_{a_1}$ ) the dashed curve is followed, rather than the curve established for annealing from the initial state at  $T_{a_2}$  only.

Table I gives a summary of these phenomena and the property changes that have been used in experimental studies. The references given are representative of a wider literature on the subject.

Complications to the above classifications often arise. Scott *et al.* [4] pointed out that “ln  $t$ ” kinetics are not obeyed over the whole time–temperature regime when observing stress relaxation in a bend test (strain at constant stress). The breakdown occurs in the early stages of relaxation which are experimentally detectable at short annealing times and low annealing temperatures, and in the late stages of relaxation which are most conveniently studied at high annealing temperatures. Breakdown of “ln  $t$ ” kinetics is also seen in the usual time–temperature ( $t$ – $T$ ) regime if the specimens are annealed before performing the bend test [4]. For a reversibility experiment Chen reported [9] that by choosing a suitable ( $t$ – $T$ ) regime in measurements of Curie temperature, an irreversible property change can be observed superimposed on a reversible change.

### 1.1. Models for relaxation in the literature

Any model for relaxation in metallic glasses must

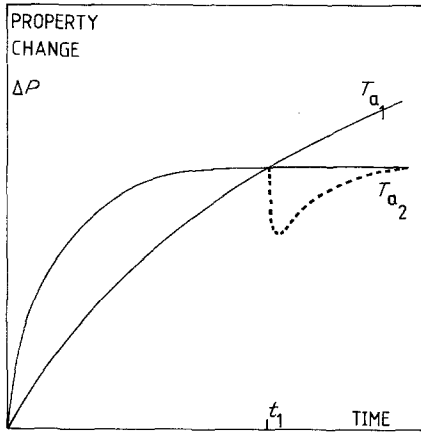


Figure 1 A schematic representation of the experimentally observed "crossover" effect. The property change,  $\Delta P$ , is plotted as a function of time,  $t$ , for two different annealing temperatures,  $T_{a1}$  and  $T_{a2}$  ( $T_{a2} > T_{a1}$ ).

account for "ln  $t$ " kinetics under certain conditions, and conversely its failure in others; it must also incorporate reversibility and crossover effects. Ideally it should relate in some way to the structural features of the material. It should be noted that "reversibility" and "crossover" effects are found in oxide glasses [10] and therefore the model should be based on some general property of the amorphous state.

Boesch *et al.* [10] studied the crossover effect in a  $B_2O_3$  glass and Greer and Leake [3] extended this work to the  $Fe_{80}B_{20}$  metallic glass. The data were fitted using a two-relaxation time model of the form

$$P(t) = A_0 \pm [A_1 \exp(-t/\tau_1) + A_2 \exp(-t/\tau_2)], \quad (1)$$

where  $P(t)$  is the measured property,  $A_0$ ,  $A_1$  and  $A_2$  are constants and  $\tau_1$  and  $\tau_2$  are characteristic relaxation times. Cost and Stanley [7] used a similar approach in studying the reversibility of resistivity of an  $Fe_{40}Ni_{40}P_{14}B_6$  metallic glass. In

this case four characteristic relaxation times were required to fit the data. There are, however, fundamental problems in relating the constants and characteristic relaxation times to physical properties of the material.

Egami [6] approached the problem of the "ln  $t$ " kinetics found for the change in the second peak of the X-ray diffraction pattern on annealing by assuming that the relaxation rate has an activation energy related linearly to the instantaneous magnitude of the measured property. Thus

$$\frac{dx}{dt} = B \exp\left(\frac{-\alpha x}{kT}\right), \quad (2)$$

where  $x$  is the relaxing quantity, and  $B$  and  $\alpha$  are constants. By allowing for the initial condition of the glass before the start of the experiment Egami was able to fit his "ln  $t$ " data. By including a back flux of processes as well as the forward flux described by Equation 2 it is possible to achieve stabilization of a measured property (i.e.  $dx/dt = 0$ ) on isothermal annealing for sufficient time [11]. However, it is not obvious why the activation energy should be related in this way to the measured property.

The third approach to relaxation kinetics has been to consider a spectrum of activation energies. Argon and Kuo [12] and Woldt and Neuhäuser [13] studied anelastic load relaxation in metal-metal and metal-metalloid metallic glasses. The data are analysed according to an expression of the form [13]

$$P = P_\infty + \sum_i P_i \exp\left(\frac{-t}{\tau_i}\right), \quad (3)$$

where  $P_\infty$  and  $P_i$  are constant and where in this case the  $\tau_i$  are assumed to obey an Arrhenius-type expression of the form

$$\tau_i = \tau_0 \exp\left(\frac{E_i}{kT}\right), \quad (4)$$

TABLE I A representative summary of experimental work on relaxation phenomena

ln $t$	Reversibility	Crossover
Curie temperature [1]	Curie temperature [2]	Curie temperature [3]
Young's modulus [4]	Young's modulus [4]	Young's modulus [4]
Stress at constant strain [5]		
Strain at constant stress [4]		
"Structure" [6]		
Length [4]		
Resistivity [7]	Resistivity [7]	
	Magnetic anisotropy [8]	
	Specific heat [9]	

where  $E_i$  is the activation energy of a process having a characteristic time  $\tau_i$  for relaxation. In the case of load relaxation the weighting factors ( $P_i$ ) can be related to structural properties of the specimen [13]. Argon and Kuo [12] use a more complex analysis based on the work of Primak [14] which is discussed below.

From the literature, therefore, it can be seen that it is possible to fit experimental data showing one of the three relaxation phenomena given above to a model, but no one model has been able to explain the observation of all three phenomena simultaneously. Egami [15], in his computer simulations of the local structural parameters, has been able to explain qualitatively many of the observed effects, but so far this model has no predictive power nor has it yielded a tractable mathematical formalism.

## 1.2. Model for relaxation

The basis of this model has been briefly described elsewhere [16, 17]. It is assumed that the activation energies of the "processes" which are available to contribute to the observed change in property on relaxation are distributed over a continuous spectrum. The following analysis does not require any specific shape of the spectrum, nor that it be smooth. The precise details of the spectrum will vary depending on the relationship between the activated "process" and the property change being measured, and on the state of the material at the start of the experiment. Such details remain to be elucidated by experiment.

By "process" is meant any thermally activated rearrangement of single atoms or atom groups. Thus some processes may involve single atom jumps (with or without this jump affecting atoms in the close environment of the jumping atom), and other processes involve the collective motion of larger groups of atoms.

## 2. Introduction of spectrum parameters

Fig. 2 is a schematic representation of one possible form of spectrum, the shape being similar to that found by Argon and Kuo [12].  $Q(E)$  is defined as the total number density of processes available for relaxation that have activation energy  $E$ ; hence  $Q(E)\delta E$  is the number of available processes in the energy range  $E$  to  $E + \delta E$ .

Since the available processes form a continuous distribution in space and energy a self-consistent description of  $Q(E)$  must allow for the interaction

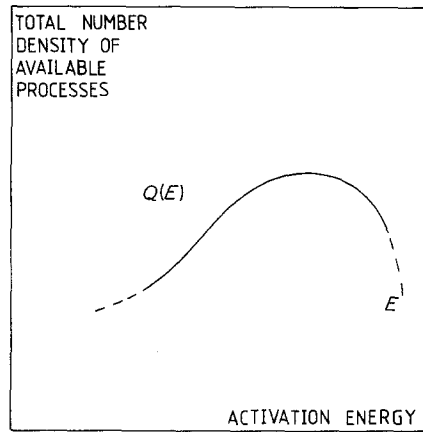


Figure 2 A schematic representation of one possible form of activation energy spectrum.

between individual relaxation processes. The treatment of relaxation in amorphous structures does not, in general, reduce to consideration of population changes in an array of isolated two-level systems with a continuous distribution of energies, since when one process is activated the resulting change in local structure changes the density of processes available for relaxation.

A more rigorous discussion of the concepts involved in defining  $Q(E)$  is given in the Appendix in the context of a model two-level activation process. Although equilibrium thermodynamics cannot be strictly applied to the relaxation of a complex metastable system, it is argued in the Appendix that if the coupling between processes is not too strong one can use the concept of a local equilibrium within a restricted energy range to deduce an equilibrium number density of available processes,  $q_s(E)$ . The equilibrium population of sites depends on Boltzmann partition and the kinetics of changes in a non-equilibrium number density depends on a chemical rate equation. The temperature dependence of  $q_s(E)$  is of importance for explaining the occurrence of "reversibility" and "crossover" in relaxing systems (see Section 7).  $q_s(E)$  clearly increases with temperature. It is possible that  $q_s(E)$  for a given  $E$  and temperature  $T$  may show a long-period time-dependence due to relaxation processes with higher values of  $E$ . In the following analysis  $q_s(E)$  is assumed to be time-independent. Finally, a quantity  $q(E)$  is defined as expressing the extent to which a structure is out of equilibrium at a given temperature:  $q(E)$  is the excess or deficit of available processes as compared to the equilibrium density,  $q_s(E)$ .

Thus generally at a given temperature,  $T$ ,

$$Q(E) = q(E) + q_s(E). \quad (5)$$

It can be seen, therefore, that at a given  $T$  it is the processes whose number density is  $q(E)$  which give rise to the observed relaxation of a physical property. The definitions of  $Q(E)$ ,  $q_s(E)$  and  $q(E)$  are further illustrated in Fig. 3. A simple form is taken for the spectrum for clarity of presentation.

The thermal activation of processes of type  $q(E)$  cannot be measured directly, only their contribution to some measured property change,  $\delta P$ . Now

$$\delta P = p(E) dE = c(E)q_t(E) dE, \quad (6)$$

where  $p(E)$  is the property change related to relaxation processes having activation energies in the range  $E$  to  $E + dE$ ;  $q_t(E)$  is the number density of processes of activation energy  $E$  which have contributed to the relaxation after time  $t$  and  $c(E)$  is the measured property change if only one such process having activation energy  $E$  is thermally activated per unit volume of material. In practice more than one type of single atom or multi-atom process may have the same value of activation energy; the value of  $c(E)$  will then depend on the type of process occurring with that value of  $E$ . The consequence of having more than one type of process each contributing to a different extent to the particular measured property is discussed

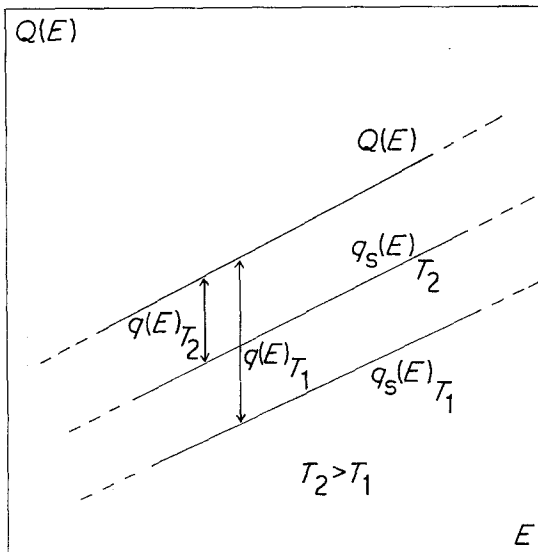


Figure 3 A schematic representation of the spectrum parameters  $Q(E)$ ,  $q(E)$  and  $q_s(E)$ , and their interrelation. The spectrum is shown in the form of straight lines for clarity.

in the Appendix. One may usually, without loss of generality, regard the processes as being all of one type with a single average value of  $c(E)$ .

The total change in the measured property,  $\Delta P$ , is given by

$$\Delta P = \int_0^E p(E) dE. \quad (7)$$

If  $q_t(E)$  can be expressed in terms of a chemical rate equation (see Appendix), then

$$q_t(E) = q(E) \left\{ 1 - \exp \left[ -\nu_0 t \exp \left( \frac{-E}{kT} \right) \right] \right\}. \quad (8)$$

This equation assumes first-order reaction kinetics, the main conclusions of the analysis being unaffected by the choice of order. The frequency factor,  $\nu_0$ , is of the order of the Debye frequency, ( $\nu_0 \approx 10^{12} \text{ sec}^{-1}$ ), for single atom processes, but may be rather different for processes involving the cooperative motion of large groups of atoms. The results of the following analysis are rather insensitive to the value of  $\nu_0$ .

From Equations 8 and 6:

$$p(E) dE = p_0(E) \times \left\{ 1 - \exp \left[ -\nu_0 t \exp \left( \frac{-E}{kT} \right) \right] \right\} dE, \quad (9)$$

where  $p_0(E)$  is the total available property change in the range  $E$  to  $E + dE$  after all processes  $q(E)dE$  have contributed to the relaxation. Following Primak [14], Equation 9 can be rewritten as

$$p(E) = p_0(E) \theta(E, T, t), \quad (10)$$

where  $\theta(E, T, t)$  is defined as the characteristic annealing function. The function  $\theta(E, T, t)$  is a measure of the proportion of available processes of type  $q(E)$  at energy,  $E$ , which have contributed to the property relaxation after time  $t$  at annealing temperature,  $T$ . The form of  $\theta(E, T, t)$  is given in Fig. 4. Two points should be particularly noted:  $\theta(E, T, t)$  changes from 0.01 to 0.99 over a narrow range of  $E$  ( $7kT$  at 473 K for example). and if  $T$  is fixed the  $\theta(E, T, t)$  profile moves along the  $E$ -axis linearly with the logarithm of annealing time. It follows, therefore, that, if the activation energy spectrum is broad, the function  $\theta(E, T, t)$  can be replaced to a good approximation by a step function at an energy  $E_0$  [14] where

$$E_0 = kT \ln(\nu_0 t). \quad (11)$$

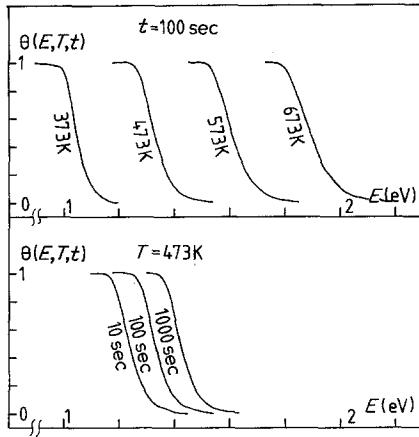


Figure 4 The functional form of the characteristic annealing function  $\theta(E, T, t)$  as it depends on time,  $t$ , and temperature,  $T$ .

For  $E < E_0$  the function has value unity, for  $E > E_0$  its value is zero. For each decade of time  $E_0$  only increases by  $2.3kT$ , and thus only a small fraction of the total spectrum may be sampled during the course of a laboratory scale isothermal annealing experiment. To illustrate this point consider the data of Mizoguchi *et al.* [1] on the changes in Curie temperature on annealing; when  $t = 10^6$  sec and (the isothermal annealing temperature)  $T = 523$  K,  $E_0 = 1.87$  eV, that is, few processes with  $E > 1.87$  eV will have contributed to the relaxation.

The approximation of  $\theta(E, T, t)$  as a step function at  $E = E_0$  is equivalent to assuming that during an isothermal anneal, at time  $t$ , all processes with  $E < E_0$  have contributed to the relaxation and all processes with  $E > E_0$  have yet to contribute.

### 3. "ln t" kinetics

In an isothermal annealing experiment with  $\theta(E, T, t)$  a step function

$$p(E) dE = p_0(E) dE = c(E) q(E) dE \text{ for } E < E_0 \quad (12)$$

$$p(E) dE = 0 \text{ for } E > E_0, \quad (13)$$

and

$$\Delta P = \int_0^{E_0} p_0(E) dE. \quad (14)$$

If  $p_0(E)$  is constant with respect to  $E$  for  $E < E_0$ ,

$$\Delta P = p_0(E) kT \ln(\nu_0 t), \quad (15)$$

and "ln t" kinetics will be observed. The assump-

tion of  $p_0(E)$  constant is discussed in Section 2.4, but is not severe as it only has to be true over the range of  $E$  swept in the experiment. It is thus possible, using this form of analysis, to demonstrate the conditions necessary for the observation or non-observation of "ln t" kinetics.

The formalism of Egami given in Equation 2 is a special case of this analysis. At any specific time,  $t$ , those processes having activation energy,  $E_0$ , will be dominating the relaxation behaviour; thus  $\alpha x = E_0$  in Equation 2,  $\alpha x$  then has the appropriate time dependence and  $\alpha$  depends on  $T$  and  $\nu_0$ .

### 3.1. Comparison with experiment

Recently, Bothe and Neuhäuser [18] have calculated the expected changes in Young's modulus on annealing an  $\text{Fe}_{32}\text{Ni}_{36}\text{Cr}_{14}\text{P}_{12}\text{B}_6$  alloy, assuming a spectrum of available processes and  $p_0(E) = \text{constant}$ . The fit to the experimental data was excellent. It remains to be seen, however, how sensitive these calculations are to the assumptions made. An analysis using the concept of an annealing function was also used successfully by Argon and Kuo [12] in their load relaxation studies.

Measurements on the coercive field of  $\text{Fe}_{40}\text{Ni}_{40}\text{B}_{20}$  after cold-rolling, which represents a measure of stress relaxation [19], are shown in Fig. 5. In the absence of pre-annealing before rolling the reduced coercive field,  $\beta$ , varies linearly with  $\ln t$  over the whole range plotted. However, pre-annealing before cold-rolling clearly removes

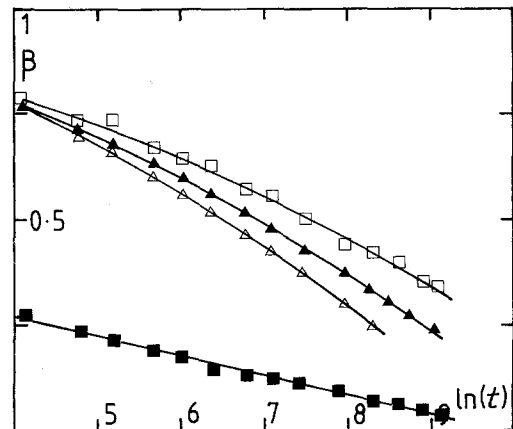


Figure 5 Reduced coercive field,  $\beta$ , plotted against  $\ln(t)$  for cold-rolled  $\text{Fe}_{40}\text{Ni}_{40}\text{B}_{20}$  annealed at 607 K to show the effects of annealing before cold-rolling. ■ cold-rolled, □ annealed for 180 sec at 648 K. ▲ annealed for 3600 sec at 607 K. △ annealed for 8100 sec at 586 K.

the “ln  $t$ ” behaviour. It should be noted that the detailed shape of the activation energy spectrum available during the final annealing treatment depends on all the stages of the thermo-mechanical history of the sample. In general, cold-rolling will create processes having a small activation energy, whereas annealing removes such processes [19]; however, the major change in Fig. 5 is due to pre-annealing prior to cold-rolling. For the three pre-annealing treatments shown it is possible to calculate the position of  $E_0$  at the end of the pre-anneal from Equation 11. For  $T_a = 648$  K and  $t = 180$  sec,  $E_0 = 1.843$  eV, for  $T_a = 607$  K and  $t = 3600$  sec,  $E_0 = 1.875$  eV, and for  $T_a = 586$  K and  $t = 8100$  sec,  $E_0 = 1.851$  eV. On subsequent annealing at 607 K after cold-rolling, “ln  $t$ ” kinetics are not expected before  $E_0$  has swept up to a region of the spectrum which was not sampled during the pre-annealing treatment (assuming that the cold-rolling has not restored the spectrum to its form before pre-annealing). For  $T_a = 607$  K this arises after times of 1640, 3600 and 2260 sec, respectively (ln  $t = 7.4$ , 8.2 and 7.7). From Fig. 5 it is clearly true that “ln  $t$ ” kinetics are not observed for times shorter than those calculated, but the data do not extend far enough to establish whether or not “ln  $t$ ” kinetics are re-established at sufficiently long annealing times.

#### 4. Isothermal annealing

The general form of the curve of measured property change,  $\Delta P$ , against time on isothermal annealing is illustrated in Fig. 6a. The interpretation in terms of a spectrum of available processes is illustrated in Fig. 6b to d. The change,  $\Delta P$ , is directly related to the shaded area through Equations 6 and 7 for each increment of annealing time. During each equal increment in  $t$  the area swept out is reduced due to the logarithmic dependence of  $E_0$  on  $t$ , and the corresponding change,  $\Delta P$ , is smaller.

For “ln  $t$ ” kinetics it has to be assumed that  $c(E)q(E)$  does not vary with  $E$  (see Section 3). The range of  $E$  for which this must hold is determined by the time range of the observations; if the observation time is doubled on a log scale the range of  $E$  of interest is only increased by  $2.3kT$  and unless  $c(E)$  or  $q(E)$  change sharply with  $E$  a curve such as Fig. 6a will be observed. The value of  $c(E)$  will depend on the type of process operating with energy  $E$  and the property being measured, the average value of  $c(E)$  and its variation with  $E$

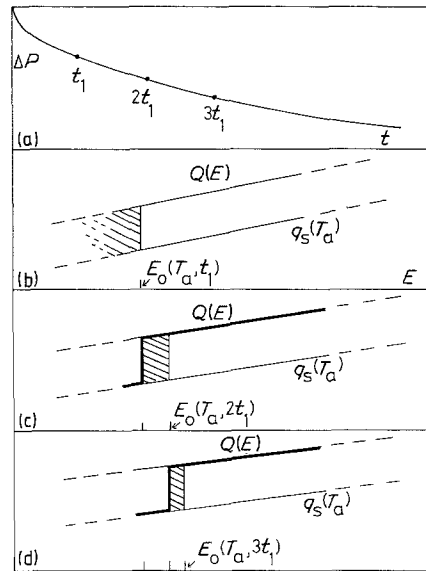


Figure 6 A schematic illustration of the often observed form of the isothermal annealing curve for property change  $\Delta P$  in terms of an activation energy spectrum. The bold line in (c) and (d) is the shape of the spectrum before these subsequent annealing periods.

will depend on the details of a specific model of structural relaxation, (e.g. relaxation of excess free volume [2], or variation of second moment of local stress [15]).

#### 5. Isochronal annealing

Greer and Spaepen [2] report the change in Curie temperature on isochronal annealing of  $\text{Fe}_{40}\text{Ni}_{40}\text{P}_{14}\text{B}_6$  and  $\text{Fe}_{80}\text{B}_{20}$  metallic glasses in the as-quenched condition. Their data are reproduced schematically in Fig. 7a, and an interpretation in terms of a spectrum of available processes is given in Fig. 7b to d. Just as in the case of isothermal annealing, the total property change is given by the changes in the spectrum induced by the heat treatment. There are both “reversible” and “irreversible” components to the spectrum and it is the combination of these components which gives rise to the form of the isochronal annealing curve. The “reversible” part comes from the temperature dependence of  $q_s(E)$  mentioned earlier. As  $T$  is increased  $q_s(E)$  will increase for any given  $E$ , so that for any annealing temperature  $T_a$  above room temperature,  $T_r$ , (the temperature at which the specimen has been stored):

$$q_s(E)_{T_a} > q_s(E)_{T_r}. \quad (16)$$

Thus immediately prior to the start of the anneal

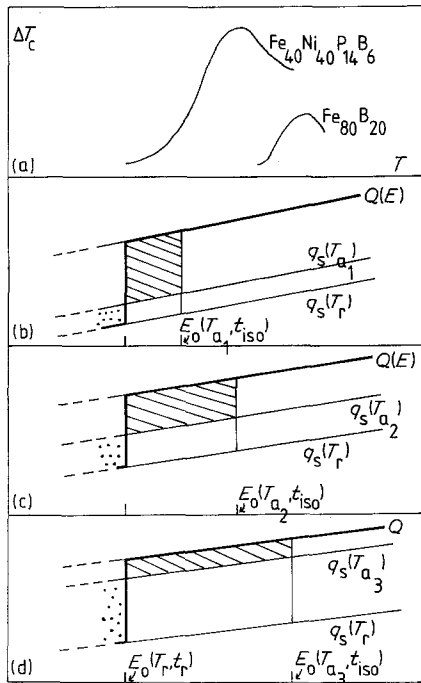


Figure 7 The isochronal annealing behaviour of  $\text{Fe}_{40}\text{Ni}_{40}\text{P}_{14}\text{B}_6$  and  $\text{Fe}_{80}\text{B}_{20}$  in terms of an activation energy spectrum (curve 7a after Greer and Spaeper [2]). The bold line in (b) to (d) represents the shape of the spectrum at the start of the anneal. The areas shown dotted are the “reversible” components of the spectrum, and the cross-hatched areas the “irreversible” components. The temperature dependence of  $q_s$  is exaggerated for clarity.

at  $T_a$  one has for all  $E < E_0(T_r, t_r)$  where  $t_r$  is the storage time at  $T_r$

$$Q(E) < q_s(E)_{T_a} \text{ or } q(E) < 0, \quad (17)$$

that is, the number of available processes,  $Q(E)$ , is less than the equilibrium number of temperature  $T_a$ . On raising the temperature to  $T_a$  these processes are reintroduced to the system as it establishes local equilibrium at  $T_a$ , giving a change in measured property in the opposite sense from that found for the activation of  $q(E)$  type processes. The “irreversible” component comes from the relaxation of those  $q(E)$  type processes which were not significantly relaxed previously at the storage temperature  $T_r$  (i.e.  $q(E)$  for  $E > E_0(T_r, t_r)$ ).

The variation of  $q_s(E)_T$  is exaggerated in Fig. 7 and in Fig. 7d it appears that the reversible component might be larger than the irreversible component. In practice, however,  $q_s(E)_T$  will not reach  $Q(E)$  for all experimentally achievable temperatures as  $Q(E)$  is determined by the initial quench and  $Q(E) \gg q_s(E)$  for small  $E$ .

The “reversible” processes are represented by the dotted area in Fig. 7b to d. The cross-hatched area represents the usual contribution to the relaxation from  $q(E)$  processes between  $E_0(T_r, t_r)$  and  $E_0(T_a, t)$  giving the expected sense of change in the measured property. The net change in measured property is given by the difference between these two contributions. Again provided that  $c(E)q(E)$  is approximately constant with  $E$  the net change in a measured property first increases then decreases as  $T_a$  is increased.

Experimentally it is observed [2] that the magnitude of the measured property change can be a function of composition and also that the peak in the isochronal annealing curve appears at a different temperature depending on composition (see Fig. 7a). The effects of composition on the magnitude of the change would be accounted for in the parameter  $c(E)$  discussed above, and the position of the maximum by the shift of the spectrum along the  $E$ -axis, some further discussion is given by Leake *et al.* [17].

The presence of a “reversible” component to the spectrum is also the origin of observed “crossover” and “reversibility” effects.

## 6. “Crossover” effects

Fig. 8a is a schematic representation of the “crossover” effect. The initial annealing treatment at temperature  $T_{a1}$  for time  $t_1$  establishes the spectrum illustrated in Fig. 8b. If the temperature is now changed to  $T_{a2}$  where  $T_{a2} > T_{a1}$ ,  $Q(E) < q_s(E)_{T_{a1}}$  for all  $E < E_0(T_{a1}, t_1)$  and these processes are restored to the system (Fig. 8d), this reverses the sense of the change in measured property giving rise to the initial sharp drop in  $\Delta P$ . For longer times  $q(E)$ -type processes are thermally activated and  $\Delta P$  changes in its original sense until the correct value for annealing at  $T_{a2}$  is achieved.

### 6.1. Comparison with experiment

Analysis of “crossover” in this way leads to certain predictions about such experiments. Up to now all “crossover” experiments have been performed by carefully annealing at the low temperature until the crossing point is reached as illustrated in Fig. 8a. A higher temperature is then chosen so that the measured property is at its saturation value for annealing at this temperature. The analysis given here predicts that “crossover” effects should be observed irrespective of the

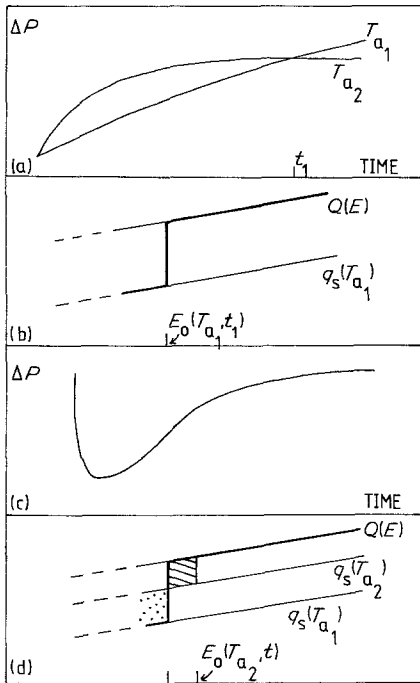


Figure 8 A schematic illustration of the "crossover" effect in terms of an activation energy spectrum. The bold line in (b) and (d) represents the spectrum established by annealing at  $T_{a_1}$  for  $t_1$ .

time of anneal at the low temperature, and irrespective of the second chosen annealing temperature.

The second prediction concerns the time at which the minimum in curve Fig. 8c occurs. This minimum cannot be achieved until a significant contribution to the relaxation is gained from  $q(E)$  process (i.e.  $E_0(T_{a_2}, t) > E_0(T_{a_1}, t_1)$ ); this occurs when

$$t \geq \frac{1}{\nu_0} \exp \left[ \frac{T_{a_1}}{T_{a_2}} \ln(\nu_0 t_1) \right]. \quad (18)$$

For the data of Greer and Spaepen [2] the times for this condition to be fulfilled are  $t = 8.3, 35$  and  $264$  sec for annealing at 673, 653 and 633 K after an initial anneal at 573 K. The position of the upturn in terms of the two-relaxation time model can be calculated to be at  $t = 5.1, 24.5$  and  $163$  sec for the final anneals at 673, 753 and 633 K, respectively. The agreement is good except for the anneal at 633 K where the minimum in the two-relaxation time model is at smaller  $t$  than calculated here. Part of this discrepancy may lie in the choice of  $\nu_0 = 10^{12} \text{ sec}^{-1}$  in the calculations. If  $\nu_0 = 10^{14} \text{ sec}^{-1}$  then the calculated times on

this model are 4.2, 19.7 and 170 sec, in much closer agreement with the two-relaxation time model.  $\nu_0 = 10^{14} \text{ sec}^{-1}$  is still a reasonable value and, as indicated above, the choice of  $\nu_0$  does depend on the process operating.

The third prediction is that the shape of the relaxation curve beyond the minimum for annealing at  $T_{a_2}$  should be identical to the relaxation curve that would be obtained if the whole annealing had been done at  $T_{a_2}$ . This is a direct consequence of the fact that all processes with  $E > E_0(T_{a_1}, t_1)$  are largely unaffected by the anneal at  $T_{a_1}$  and give their normal contribution to the relaxation at  $T_{a_2}$ . Data of Greer and Spaepen [2] are replotted in Fig. 9 to test this prediction. Within the experimental limitations the curve for annealing at  $T_{a_2}$  after the anneal at  $T_{a_1}$  is indeed independent of the pre-anneal.

## 7. "Reversibility"

Fig. 10 shows a schematic presentation of "reversibility". The dotted and shaded areas have the same meaning as above in terms of "reversible" and "irreversible" components. The first anneal at  $T_{a_1}$  for time  $t_1$  establishes the spectrum shown in Fig. 10b and the measured property change follows part 1 of curve 10a. If the temperature is now stepped to  $T_{a_2}$  ( $T_{a_2} > T_{a_1}$ ), then for all  $E < E_0(T_{a_1}, t_1)$ ,  $Q(E) < q_s(E)_{T_{a_2}}$  and these processes are restored to the system to establish the equilibrium number density. If the choice of time  $t_2$  at  $T_{a_2}$  is such that  $E_0(T_{a_2}, t_2) > E_0(T_{a_1}, t_1)$  then a significant "irreversible" component of relaxation is superimposed on the "reversible" component, (see Fig. 10c). If  $E_0(T_{a_2}, t_2) < E_0(T_{a_1}, t_1)$  then the measured property change

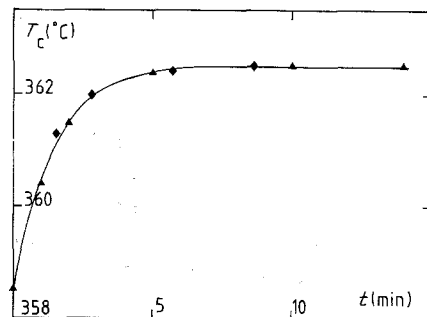


Figure 9 Data of Greer and Spaepen [2] on the "crossover" effect replotted to illustrate that the form of the curve is unaffected by the pre-annealing.  $\blacktriangle$  annealed from as-received at 673 K.  $\blacklozenge$  annealed at 673 K after pre-anneal at 573 K for 1500 sec.



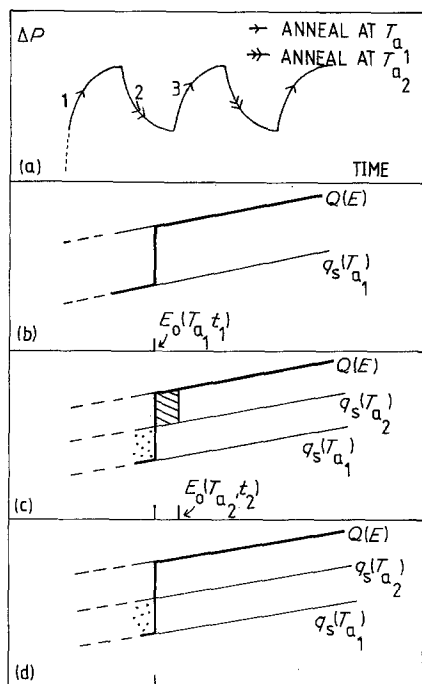


Figure 10 A schematic illustration of "reversibility" effects in terms of an activation energy spectrum. The bold line in (b) to (d) represents the spectrum established by the first anneal at  $T_{a1}$ .

on part 2 of curve 10a will be almost entirely "reversible" in nature (see Fig. 10d). On returning the temperature to  $T_{a1}$  (part 3 of curve 10a) all the processes which were restored to the system by raising the temperature to  $T_{a2}$  can now be removed as  $q_s(E)_{T_{a1}} < q_s(E)_{T_{a2}}$ . Only if the time at  $T_{a1}$  on part 3 of curve 10a is short compared to  $t_1$  (i.e.  $E_0(T_{a1}, t_1 + t) \approx E_0(T_{a1}, t_1)$ ) will the final value on this second anneal at  $T_{a1}$  be the same as at the end of the initial anneal at  $T_{a1}$ . If  $t_1 + t \gg t_1$  then a further "irreversible" component will be added to the relaxation at  $T_{a1}$ .

## 8. Conclusions

A new model has been presented for relaxation in metallic glasses, which has applicability to other amorphous systems such as oxide glasses. Comparison of the model with isothermal, isochronal, "crossover" and "reversibility" data shows an overall consistency in the approach. There is considerable scope for development and refinement using experimental techniques. The analysis given here, for the first time in this field, gives quantitative expressions which can easily be used to predict experimental relaxation behaviour. An immediate understanding of all the main features

of experimental data on relaxation can be obtained through the application of Equation 11.

## Acknowledgements

We acknowledge much useful discussion with E. Woldt, in particular with reference to the Appendix. Discussion with Professor H. Neuhäuser and K. Bothe is also acknowledged. Thanks are due to Professor R. W. K. Honeycombe for his active interest in this field of study. Part financial support from the Science and Engineering Research Council is also acknowledged. Finally, our grateful thanks to Mrs E. Palmer for meticulous typing of the manuscript.

## Appendix

Consider the population of an assembly of model double wells of form depicted in Fig. A1. The double wells are considered initially to be isolated and represent a particular structural configuration which permits an atom to be either in a higher energy position at level  $E_1$  or in a lower energy position at  $E_2$ . In a real amorphous structure there will be a spectrum of more complex strongly coupled wells with each atom able to jump to a number of different positions at differing energies, the action of jumping changing the levels of neighbouring wells.

Considering the population of the system of isolated wells, if there are  $n_1$  atoms at  $E_1$  and  $n_2$  atoms at  $E_2$  we may define a local equilibrium (neglecting coupling to other systems of wells) with  $n_1 = n_1^s$  and  $n_2 = n_2^s$  by the condition

$$\frac{dn_1^s}{dt} = \frac{dn_2^s}{dt} = 0. \quad (\text{A1})$$

Now the general chemical rate equation gives

$$\frac{dn}{dt} = \nu n^\alpha \quad (\text{A2})$$

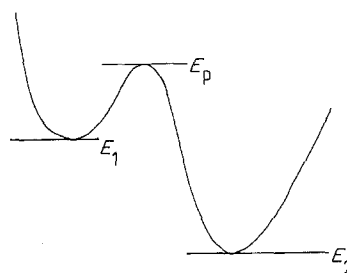


Figure A1 A schematic illustration of a model double well potential in an amorphous material.

where

$$\nu = \nu_0 \exp(-E/kT) \quad (\text{A3})$$

and  $\alpha$  is the order of the reaction. Assuming  $\alpha = 1$  we have

$$\left. \frac{dn}{dt} \right|_{1 \rightarrow 2} = -n_1 \nu_0 \exp[-(E_p - E_1)/kT] \quad (\text{A4})$$

$$\left. \frac{dn}{dt} \right|_{2 \rightarrow 1} = -n_2 \nu_0 \exp[-(E_p - E_2)/kT] \quad (\text{A5})$$

whence in equilibrium

$$n_1^s/n_2^s = \exp[-(E_1 - E_2)/kT], \quad (\text{A6})$$

which is an expression of Boltzmann partition over the energy levels in equilibrium.

In terms of the model proposed  $n_1 = Q(E) dE$  the number of available processes for relaxation and  $E = (E_p - E_1)$ . A condition of local equilibrium can be defined if the various structural processes are sufficiently isolated. At equilibrium  $n_1^s = \int q_s(E) dE$ . Also  $n_1 - n_1^s = \int q(E) dE$  when the system is not in equilibrium. For the assembly of double wells  $n_1 + n_2$  is constant so that,

$$n_1 = n_1^s + \int q(E) dE \quad (\text{A7})$$

$$n_2 = n_2^s - \int q(E) dE,$$

whence

$$\left. \frac{dn}{dt} \right|_{1 \rightarrow 2} = -n_1^s \nu_0 \exp[-(E_p - E_1)/kT] - \int q(E) dE \nu_0 \exp[-(E_p - E_1)/kT] \quad (\text{A8})$$

$$\left. \frac{dn}{dt} \right|_{2 \rightarrow 1} = -n_2^s \nu_0 \exp[-(E_p - E_2)/kT] - \int q(E) dE \nu_0 \exp[-(E_p - E_2)/kT].$$

From Equation A6,

$$n_1^s \nu_0 \exp[-(E - E_1)/kT] = n_2^s \nu_0 \exp[-(E - E_2)/kT],$$

so that

$$\begin{aligned} \frac{dn_1}{dt} = -\frac{dn_2}{dt} = -q(E) dE \nu_0 \\ \times \{(\exp[-(E_p - E_1)/kT] \\ + \exp[-(E_p - E_2)/kT])\}. \end{aligned} \quad (\text{A9})$$

For  $(E_1 - E_2) \gg kT$  and  $E = (E_p - E_1)$ ,

$$\frac{dn_1}{dt} \simeq -q(E) dE \nu_0 \exp(-E/kT). \quad (\text{A10})$$

We have the important result that the rate of relaxation towards equilibrium is determined by  $E = (E_p - E_1)$  whether the approach to equilibrium is from above or below (i.e. whether  $q(E)$  is positive or negative). Substituting for  $n_1$  in Equation A10

$$\frac{dQ(E)}{dt} = -q(E) \nu_0 \exp(-E/kT), \quad (\text{A11})$$

whence, under isothermal conditions,

$$\frac{dq(E)}{dt} = -q(E) \nu_0 \exp(-E/kT). \quad (\text{A12})$$

Integrating

$$[\ln q(E)]_{q_0(E)}^{q(E)} = [-\nu_0 t \exp(-E/kT)]_0^t, \quad (\text{A13})$$

where  $q_0(E)$  is the value of  $q(E)$  at some arbitrary  $t = 0$  thus

$$q(E) = q_0(E) \exp[-\nu_0 t \exp(-E/kT)]. \quad (\text{A14})$$

Now in terms of the model the number of available processes activated or relaxed after time  $t$  is denoted by  $q_t(E) = q_0(E) - q(E)$  whence

$$q_t(E) = q_0(E) \{1 - \exp[-\nu_0 t \exp(-E/kT)]\}. \quad (\text{A15})$$

This is a direct expression of Equation 8 in Section 2.1, thus giving a quantitative basis to the model described under the restrictive assumptions made above.

If the assumptions are progressively relaxed, various complications have to be addressed:

(1) it is probable that there will be different types of double well with different values of  $E_1$  and  $E_2$  but the same value of  $E = (E_p - E_1)$ . In terms of the model there will be different "types" of "process" with the same activation energy. Each type of process will contribute to the relaxation of the property being measured in a characteristic way, in other words the value of  $c(E)$  will depend on the type of process. If Equation A14 is valid for each type of process then a simple average  $\langle c(E) \rangle$  can be used in place of  $c(E)$ ;

(2) if  $(E_1 - E_2) \lesssim kT$  the full expression

Equation A9 for the approach to equilibrium must be used, this depends on  $(E_p - E_2)$  also;

(3) in a real amorphous structure each atom must be considered as in a complex energy well with a number of possible jump directions determined by the immediate nearest neighbour configurations. Furthermore, well systems involving the activated motion of groups of atoms have also to be considered. The well systems are coupled in the sense that any atom jump changes the nearest neighbour configuration and therefore well structure relating to nearby atoms. It is likely, however, that the various activation barrier heights will be evenly distributed in space, a process involving a low activation energy being surrounded by processes with relatively high activation energies. This tendency will reduce the effective coupling between wells at a given energy and favour the establishment of the local equilibrium described by Equation A6. Over very long times, however, the state of "local equilibrium" is likely to drift towards a state of lower overall energy;

(4) when a process is activated it changes the number density distribution of available processes. For example, a low-energy jump to reduce a large excess free volume could create two or more smaller regions of excess free volume which are then new available processes at a higher energy. Although an added complication, this does not substantially alter the model described (Primak [14] also discusses the effect of "successive reactions"). The relevant  $q(E)$  value for property relaxation is that pertaining when  $E$  is within a few  $kT$  of the energy in question. An activation energy spectrum deduced from relaxation measurements will clearly include processes added to an evolving spectrum at earlier stages in the relaxation cycle.

## References

1. T. MIZOGUCHI, H. KATO, N. AKUTSU and S. HATTA, Proceedings of the 4th International Con-

- ference on Rapidly Quenched Metals, Sendai, 1981, edited by T. Masumoto and K. Suzuki, Vol. 2 (Japan Institute of Metals, 1982) p. 1173.
2. A. L. GREER and F. SPAEPEN, *Ann. New York Acad. Sci.* **371** (1981) 218.
3. A. L. GREER and J. A. LEAKE, *J. Non-Cryst. Solids* **33** (1979) 291.
4. M. G. SCOTT, R. W. CAHN, A. KURSUMOVIĆ, E. GIRT and N. B. NJUHOVIĆ, Proceedings of the 4th International Conference on Rapidly Quenched Metals, Sendai, 1981, edited by T. Masumoto and K. Suzuki, Vol. 2 (Japan Institute of Metals, 1982) p. 469.
5. E. WOLDT, Diploma, Institut A für Physik der Technischen Universität Carolo-Wilhelmina, Braunschweig (1980).
6. T. EGAMI, *J. Mater. Sci.* **13** (1978) 2587.
7. J. R. COST and J. T. STANLEY, *Scripta Metall.* **15** (1981) 407.
8. W. CHAMBRON and A. CHAMBEROD, *Sol. Stat. Commun.* **33** (1980) 157.
9. H. S. CHEN, *J. Appl. Phys.* **52** (1981) 1868.
10. L. BOESCH, A. NAPOLITANO and P. B. MACEDO, *J. Amer. Ceram. Soc.* **53** (1970) 148.
11. D. KUHLMANN, *Z. Physik* **124** (1948) 468.
12. A. S. ARGON and H. Y. KUO, *J. Non-Cryst. Solids* **37** (1980) 241.
13. E. WOLDT and H. NEUHÄSER, *J. Phys. C8* **41** (1980) 846.
14. W. PRIMAK, *Phys. Rev.* **100** (1955) 1677.
15. T. EGAMI, *Ann. New York Acad. Sci.* **371** (1981) 238.
16. M. R. J. GIBBS and J. E. EVETTS, Proceedings of the 4th International Conference on Rapidly Quenched Metals, Sendai, 1981, edited by T. Masumoto and K. Suzuki, Vol. 2, (Japan Institute of Metals, 1982) p. 479.
17. J. A. LEAKE, M. R. J. GIBBS and J. E. EVETTS, *ibid.*, p. 513.
18. K. BOTHE and H. NEUHÄUSER, *Scripta Metall.* submitted.
19. M. R. J. GIBBS, Proceedings of the Conference on Metallic Glasses Science and Technology, Budapest, 1980, edited by C. Hargitai, I. Bakonyi and T. Kemeny, Vol. 2 (Central Research Institute for Physics, Budapest, 1980) p. 37.

Received 5 April  
and accepted 2 July 1982